

Supplementary Material

S1. Nanoparticle surface self-diffusion

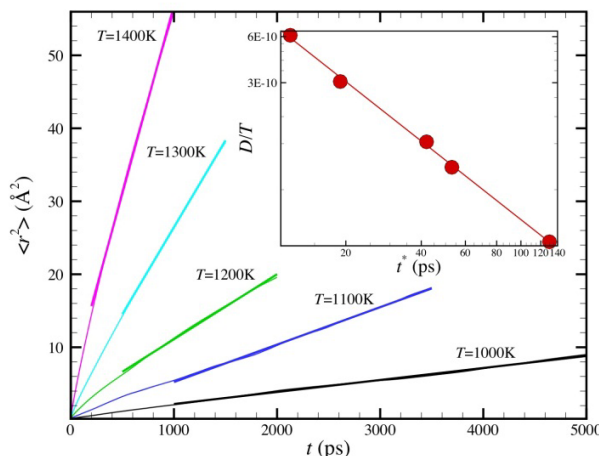


Figure S1. Mean squared displacement of interfacial region atoms as a function of simulation time in $N = 2899$ NP for five different temperatures. The inset shows the log-log plot of Ni atom self-diffusivity D / T in the interfacial region versus diffusion decorrelation time or ‘string lifetime’, t^* .

S2. String Fractal Dimension

The strings within the interfacial layer of the NP can be expected to be somewhat different than bulk glass forming liquids due to the normally thin nature of the interfacially mobile layer. At low temperatures this layer must reduce to a single layer of atoms and the chains would see a locally two-dimensional environment. Simulations of the string dimensions of strings in bulk GF polymer liquids has recently revealed that the scaling properties of the strings can be very well described as self-avoiding where the radius of gyration of the chains scales as a power ν of the chain length that is close to $\nu = 3/5$, the well known exponent for self-avoiding walks (SAWs) in three spatial dimensions.¹ We also found string-like collective motion in association with the homogeneous melting of bulk Ni where again ν was found to be close to $3/5$.² Reducing the spatial dimension to two dimensions makes the SAW exponent increase to the exact value, $3/4$ so we expect the exponent to grow upon cooling since the interfacial layer of the NP gets

progressively thin upon cooling. We indeed see this expected trend in our string data shown in Fig. S.2, where the apparent exponent ν instead seems to be approaching a value near 1, an exponent more in line the Ising model in two dimensions and stiff worm-like chains. The critical exponent for continuous symmetry phase transition models such the KT model, which belongs to the XY model universality class where $\nu \approx 2/3$ in three dimensions), goes to infinity upon approaching two dimensions. Although the full significance of the value of this apparent ν is not clear at present, it is clear that the increasing confinement of the interfacial layer of the NP is increasing the effective value of ν upon cooling.

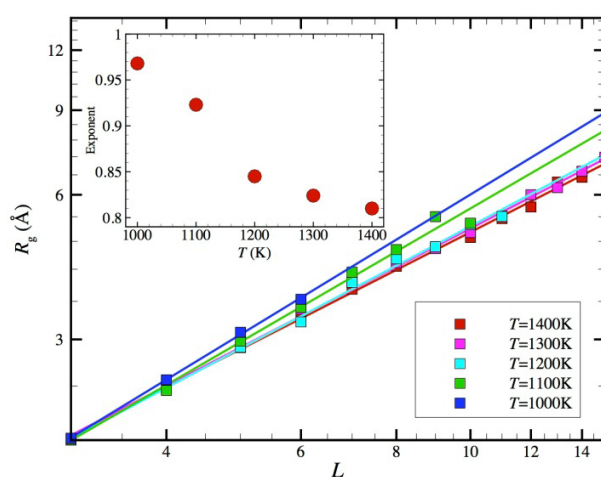


Figure S2. Scaling of string size with string length, $R_g \sim L^\nu$ where the inset shows $\nu = 1 / d_f$ as a function of T . The fractal dimension d_f seems to be approaching a value near 1, corresponding to highly persistent worm-like chains.

S3. Self-intermediate Scattering Function

The self-intermediate scattering function $I(\mathbf{q}, t) = \langle \exp\{-i\mathbf{q}[\mathbf{r}_i(t) - \mathbf{r}_i(0)]\} \rangle^3$ for the interfacial atomic motion is simply the Fourier transform of the atomic displacement distribution function $G_s(\mathbf{r}, t)$ (The Fourier transform variable \mathbf{q} is often termed the scattering ‘wave vector’.) After exhibiting a plateau associated with the particle caging phenomenon, $I(\mathbf{q}, t)$ in GF liquids

normally exhibits a ‘stretched exponential’ variation, $I(q,t) \propto \exp[-(t/\tau)^{\beta_s}]$. Our interfacial relaxation data for $I(q,t)$ exhibits this same trend (illustrated in Figure S3) where the ‘stretching exponent’ β_s determined from our fits to this equation is rather insensitive to T , i.e., $\beta_s = 0.36 \pm 0.02$. In our NP system, it is clear that cannot be taken as a measure of collective atomic motion.

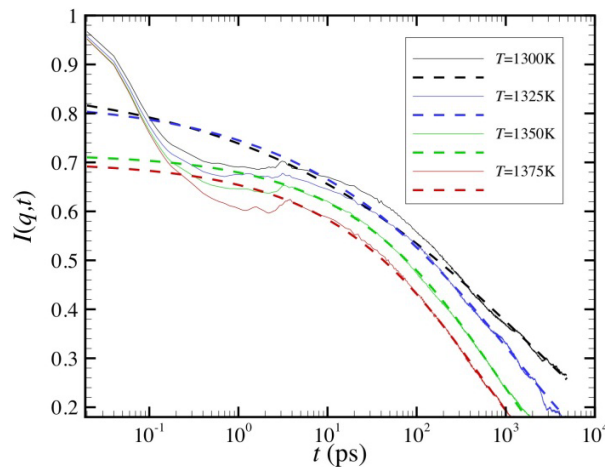


Figure S3. The self-intermediate scattering function for interfacial NP dynamics in the T range of 1300 K and 1375 K and for $N=2899$. The dashed curves are a fit⁵ to stretched exponential equation, $I(q,t) \propto \exp[-(t/\tau)^{\beta_s}]$.

S4. Sutton-Chen Potential

In the Sutton-Chen form of EAM potential, the total internal energy of pure metals was expressed in terms of Finnis-Sinclair form, as follows:

$$E = \varepsilon \left[\frac{1}{2} \sum_{i \neq j} \sum V(r_{ij}) - c \sum_i \sqrt{\rho_i} \right] \quad (\text{S1})$$

where $V(r) = (a/r)^n$ is the pair potential and $\rho_i = \sum_{j \neq i} (a/r_{ij})^m$ is the electron density function.

Here, r_{ij} is the spacing between atoms i and j , c is a positive dimensionless parameter, ε is a

parameter with unit of energy, a is the lattice parameter and m and n are positive integers. The parameters ε , c , m and n as well as lattice parameter a and cohesive energy E_c for Ni, Ag, Au and Pt are listed in Table 1.

Table 1 Potential parameters for pure fcc metals Ni, Ag and Pt^{4,5}

	ε (eV)	c	m	N	A	E_c (eV)
Ni	1.5713×10^{-2}	39.755	6	9	3.52	4.44
Ag	2.5415×10^{-3}	145.658	6	12	4.09	2.96
Au	1.2794×10^{-2}	34.428	8	10	4.08	3.78
Pt	1.9835×10^{-2}	34.428	8	10	3.92	5.86

For an A-B alloy system, parameters ε^{AA} , c^{AA} , m^{AA} , n^{AA} , a^{AA} and ε^{BB} , c^{BB} , m^{BB} , n^{BB} , a^{BB} are simply taken with the parameters of pure A metal and pure B metal from Table 1, respectively. A simple arithmetic and geometric means are employed to estimated the parameters for A-B interactions,

$$\begin{aligned}
 m^{AB} &= \frac{1}{2}(m^{AA} + m^{BB}) \\
 n^{AB} &= \frac{1}{2}(n^{AA} + n^{BB}) \\
 a^{AB} &= (a^{AA}a^{BB})^{1/2} \\
 e^{AB} &= (e^{AA}e^{BB})^{1/2}
 \end{aligned} \tag{S2}$$

Since the sensitivity of simulation results to the choice of atomic potential is important in comparisons of simulations to measurements and the extent of collective motion L is a primary variable in our analysis, we examine how the choice of atomic potential affects simulation estimates of the temperature dependence of the extent of collective motion L in our simulations

in Fig. S4. A comparison between the Voter-Chen and Sutton-Chen EAM potential models for Ni shows only a relative small difference in L estimates as a function of T when the results are compared on a reduced temperature scale, T / T_m , where T_m is the melting temperature of the NP with the same number of atoms and computed by the same method. On the other hand, the melting temperatures found for these two Ni potentials lead to melting temperatures differing by 450 K! We suggest that a greater transferability of the results between different potential models by expressing results in reduced rather than absolute temperature scales. Basically, this procedure corresponds to an appeal to equation of state reasoning.

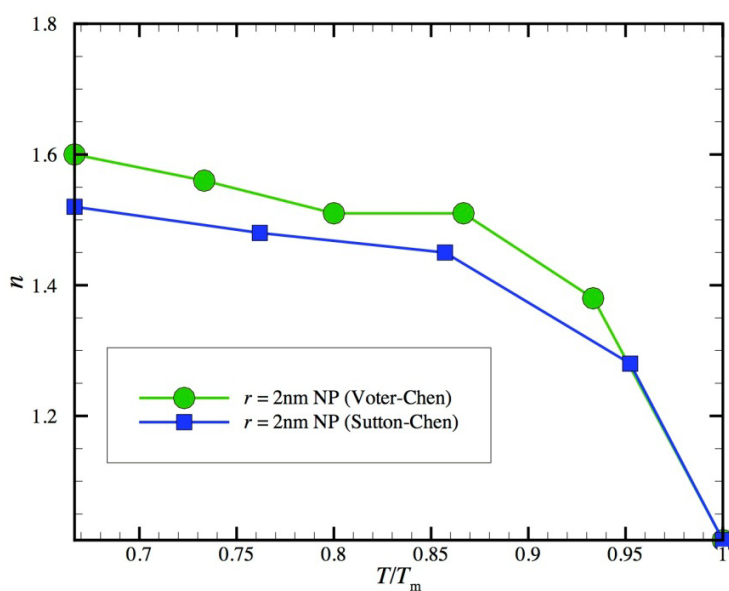


Figure S4. Comparison of T dependence of string length of $N = 2899$ Ni NP using Voter-Chen and Sutton-Chen EAM potential. For the $N = 2899$ and $r = 2$ nm Ni NP, Voter-Chen estimates the melting temperature T_m to be $T_m \approx 1500$ K, while Sutton-Chen predicts at $T_m \approx 1050$ K. Despite the large discrepancy in the predicted T_m for these potentials, the T dependence of L , when expressed in a reduced temperature scale, is rather independent of the choice of potential.

S5. Van Hove Correlation Function

The self-part of the van Hove correlation function $G_s(r, \Delta t)$ describes the probability distribution of the position r of an atom after a time Δt . Mathematically, the van Hove correlation function can be written as:

$$G_s(\mathbf{r}, \Delta t) = \frac{1}{N} \left\langle \sum_{i=1}^N \delta(\mathbf{r}_i(\Delta t) - \mathbf{r}_i(0) - \mathbf{r}) \right\rangle. \quad (\text{S3})$$

When Δt is small, $G_s(r, \Delta t)$ is Gaussian, meaning the atom undergoes harmonically localized motion. As the time interval Δt increases, generally we expect to observe non-Gaussian behavior. By looking at $G_s(r, \Delta t)$ at different time intervals, we can trace the path that the atom takes as it moves through the system and quantify these changes in terms of atomic displacement.

Figure S5 shows the self-part of the van Hove correlation function of $N = 2899$ NP at $T = 1400$ K with $\Delta t = 20$ ps. The displacement for each atom has been resolved into two components, the displacement along radial direction \mathbf{r}_{\parallel} and the displacement perpendicular to the radial direction \mathbf{r}_{\perp} . As discussed in above, the multiple peaks centering at successive nearest-neighbor distances in $G_s(r)$ implies a ‘hopping’ motion to preferentially quantized distances. These hopping peaks are very pronounced as in the present simulations for two-dimensional fluids exhibiting hexatic ordering.⁶ However, this feature disappears when the temperature arises above the melting point, as shown in the inset. Since mobile atoms predominantly occur on the NP surface, it is perhaps not surprising to see that the displacement perpendicular to the radial direction is the major contribution to the overall atomic displacement.

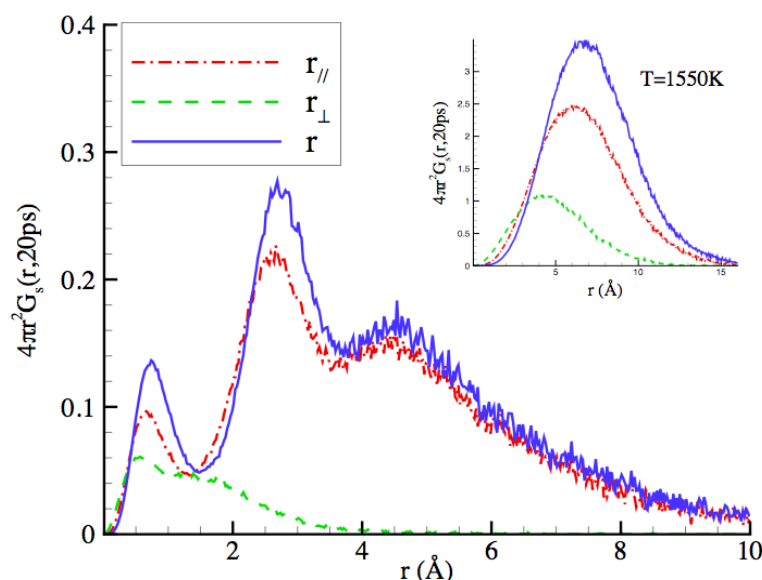


Figure S5. The self-part of the van Hove correlation function of $N = 2899$ NP at $T = 1400\text{K}$ with $\Delta t = 20$ ps. The inset shows $G_s(r, \Delta t)$ of the same NP at $T = 1550\text{ K}$.

References

- 1 K. F. Freed, http://home.uchicago.edu/_freed/.
- 2 H. Zhang and J. F. Douglas, *J. Chem. Phys.*, 2012, accepted.
- 3 J. P. Hansen and I. R. McDonald, *Theory of Simple Liquids*, Academic, London, New York, 2nd edn, 1986.
- 4 A. P. Sutton and J. Chen, *Philos. Mag. Lett.*, 1990, **61**, 139–146.
- 5 H. Rafiitabar and A. P. Sutton, *Philos. Mag. Lett.*, 1991, **63**, 217–224.
- 6 R. Zangi and S. A. Rice, *Phys. Rev. Lett.*, 2004, **92**, 35502